



1 **Measurement report: Immediate impact of the Taal volcanic eruption**
2 **on atmospheric temperature observed from COSMIC-2 RO**
3 **measurements**

4 Saginela RavindraBabu and Yuei-An Liou

5 Center for Space and Remote Sensing Research, National Central University, Taiwan

6 * Correspondence: yueian@csrrs.ncu.edu.tw; Tel.: +886-3-4227151 (ext. 57631)

7
8 **Abstract**

9 For the first time after 43 years of its previous eruption in 1977, the Taal volcano
10 in the Philippines (14°N, 120°59'E) erupted in the afternoon of 12 January, 2020.
11 Interestingly, the Taal volcanic eruption was associated with a strong anticyclonic
12 circulation at the upper levels over the western Pacific region in the northern
13 hemisphere. As a result, the volcanic plumes were carried through the background
14 upper level strong winds to the anticyclone over the Pacific Ocean within a few days
15 following the eruption. In this study, the detailed vertical structure and the day-to-day
16 temperature variability in response to the eruption is delineated by using high-
17 resolution temperature measurements from the recently launched Constellation
18 Observing System for Meteorology, Ionosphere, and Climate (COSMIC)-2 radio
19 occultation (RO) data. We describe the vertical temperature structure near (within 2
20 degree radius) and away (~ 5 degree radius) from the volcano during its intense eruption
21 day (13 January 2020). A significant temperature inversion at ~15 km altitude is
22 observed in the nearest temperature profiles (within 2 degree radius). Multiple
23 tropopause are evident in the temperature profiles that are available away from the
24 volcano (~ 5 degree radius). The cloud top altitude of 15.2 km detected from the RO
25 bending angle anomaly method is demonstrated. Furthermore, the diurnal temperature
26 and relative humidity anomalies are estimated over $\pm 5^\circ$ latitude and longitude radius
27 from the volcano center and over the region of 10-20N, 160-180E with respect to the
28 mean temperature of one week before the eruption. A persistent warming layer is



29 observed at 16-19 km altitude range in both regions for several days after the eruption.
30 A strong increase of ~50% relative humidity at 15 km altitude is also noticed just after
31 the eruption in the Taal volcano region. The present work shows the advantages and
32 usefulness of the newly-launched COSMIC-2 data for near real-time temperature
33 monitoring at shorter time scales with sufficient data.

34 **Keywords:** Taal volcanic eruption; COSMIC-2; temperature; relative humidity

35

36 1. Introduction

37 The volcanic eruptions are dominant natural sources of the stratospheric sulfate
38 aerosols and have a strong impact on global climate (Robock, 2000, 2015). Over
39 decades, the impact of volcanic sulfate aerosols on climate has received immense
40 interest due to their strong cooling effect on the Earth's lower atmosphere and warming
41 effect on the lower stratosphere. Comprehensive overview of the impact of volcanic
42 aerosols on climate can be found in Robock (2000, 2015). It is well reported that these
43 volcanic eruptions can release and inject tremendous amount of sulfur dioxide (SO₂)
44 directly into the stratosphere. These sulfate aerosols significantly reflect the solar
45 radiation and absorb the infrared radiation, causing cooling of the troposphere and
46 heating of the stratosphere. The major volcanic eruptions, such as 'El Chichon' in 1982
47 and 'Pinatubo' in 1991, emitted large amounts of SO₂, and their impacts on global
48 climate have been discussed in several studies (e.g., Aquila et al., 2013; Free and
49 Lanzante, 2009; Randel et al., 2009). It is reported that the Pinatubo eruption in 1991,
50 caused a global tropospheric warming of up to 0.6 K and a stratospheric warming of 2
51 K for up to the first two post-eruption years (Parker et al., 1996; Robock, 2000;
52 Ramaswamy et al., 2001).

53 It is well demonstrated that the atmospheric temperatures are strongly influenced
54 by volcanic plumes. In recent decade, few studies have reported on the impact of



55 volcanic eruptions on changes in the temperature structure by using high vertical
56 resolution measurements from Global Position System (GPS) radio occultation (RO)
57 technique, relying on the high-precision measurements of atmospheric temperature by
58 the RO technique (Wang et al., 2009; Okazaki and Heki, 2012). For the first time, Wang
59 et al. (2009) and Okazaki and Heki (2012) utilized Constellation Observing System for
60 Meteorology, Ionosphere, and Climate (COSMIC) RO temperature data to study the
61 impact of volcanic eruptions on atmospheric temperature comparing RO temperature
62 data before and after the eruption. However, the reports are made by using a very less
63 number of RO data. Mehta et al. (2015) studied the impact of recent minor volcanic
64 eruptions on the upper troposphere and lower stratosphere (UTLS) temperature from
65 COSMIC RO data. Biondi et al. (2017) extensively used COSMIC RO data to detect
66 the volcanic cloud top altitude from the bending angle anomaly. Very recently, Stocker
67 et al. (2019) clearly demonstrated the importance of the small volcanic eruptions to the
68 short term temperature trends and they found that the impact of those volcanic eruptions
69 on linear trends can be up to 20%, depending on altitude and latitude. It is also reported
70 that the accurate quantification of temperature changes due to the small eruptions is
71 challenging (Stocker et al., 2019). Indeed, the detailed knowledge of the changes in the
72 vertical temperature structure due to the volcanic eruption is crucial for estimating the
73 accurate trends in the temperature as the impact of volcanic eruptions are altitude and
74 latitude dependent (Stocker et al., 2019).

75 Recently, on 12 January 2020, a large scale eruption started over the Taal volcano
76 in the Philippines (14°N 120°.59E) for the first time since 1977. At 2.30 p.m. (local
77 time), explosive eruption started and produced a giant plume of volcanic ash up to ~15
78 km in the atmosphere (Mallapaty et al., 2020). This volcanic ash further spread in the
79 northeast direction from the Taal volcano and covered the tropical Pacific Ocean in the
80 northern hemisphere (https://so2.gsfc.nasa.gov/omps_2012_now.html#2020). Based



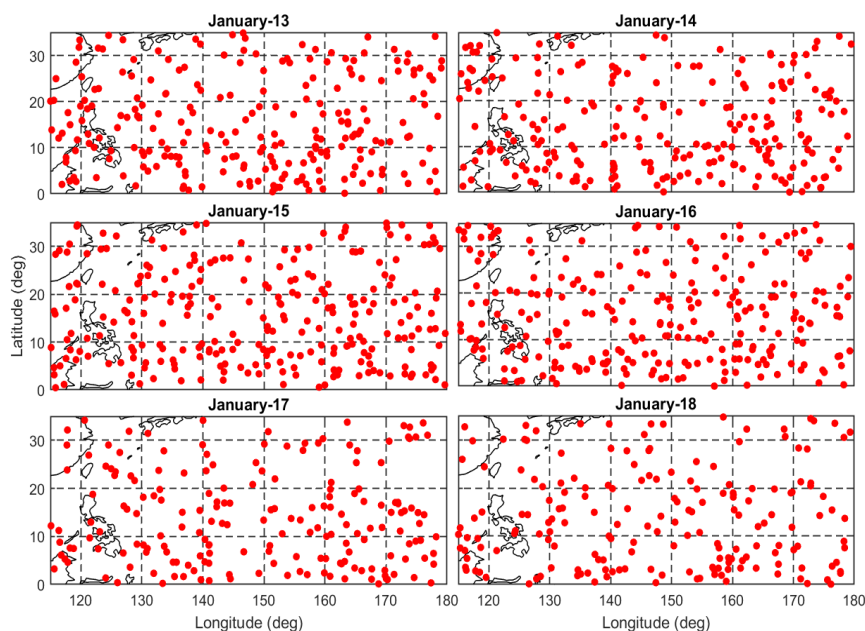
81 on Philippine Institute of Volcanology and Seismology Taal volcano bulletin reports,
82 the Taal volcanic eruption was active during 12-15 January. From 16 January onwards,
83 it has been characterized by week plume activity over the Taal main crater. In the
84 present study, we use COSMIC-2 mission RO temperature data for the first time to
85 investigate the atmospheric temperature changes due to the Taal volcanic eruption
86 during January 2020.

87

88 **2. Data Base**

89 **2.1 COSMIC-2 provisional data**

90 In the present study, high-resolution temperature profiles obtained from the
91 COSMIC-2 mission are utilized during January 2020. The COSMIC-2 mission,
92 launched on 25 June 2019, collects more than 5000 RO soundings per day over the
93 tropics and subtropics (Ho et al., 2019). The basic advantage of the COSMIC-2 mission
94 is in that it will take frequent measurements over the tropics and provide higher
95 numbers of temperature profiles in a single day compared to the previous missions due
96 to its low inclination of $\sim 24^\circ$. The data is downloaded from the COSMIC Data Analysis
97 and Archive Centre (CDAAC) website ([https://data.cosmic.ucar.edu/gnss-](https://data.cosmic.ucar.edu/gnss-ro/cosmic2/provisional/release1/level2/)
98 [ro/cosmic2/provisional/release1/level2/](https://data.cosmic.ucar.edu/gnss-ro/cosmic2/provisional/release1/level2/)). In the present study, we used wetprf
99 temperature profiles with 100 m vertical resolution. **Figure 1** shows the daily total
100 available COSMIC-2 RO profiles within the study region between 0-35N, 110-180E.
101 We have found a sufficient number of RO profiles over the study region with more than
102 200 profiles per day. The available RO profiles per day are much higher compared to
103 the other previous RO missions, including COSMIC-1. The COSMIC-2 mission will
104 give a higher density of the temperature profiles over the tropics. Hence, it is plausible
105 to study the diurnal variability of temperature and tropospheric humidity changes over
106 the tropics.



107

108 **Figure 1.** Spatial distribution of COSMIC-2 radio occultation profiles observed during
 109 13-18 January 2020 over 0-35N, 110-180E region.

110

111 2.3 Ozone Monitoring Instrument (OMI) SO₂ data

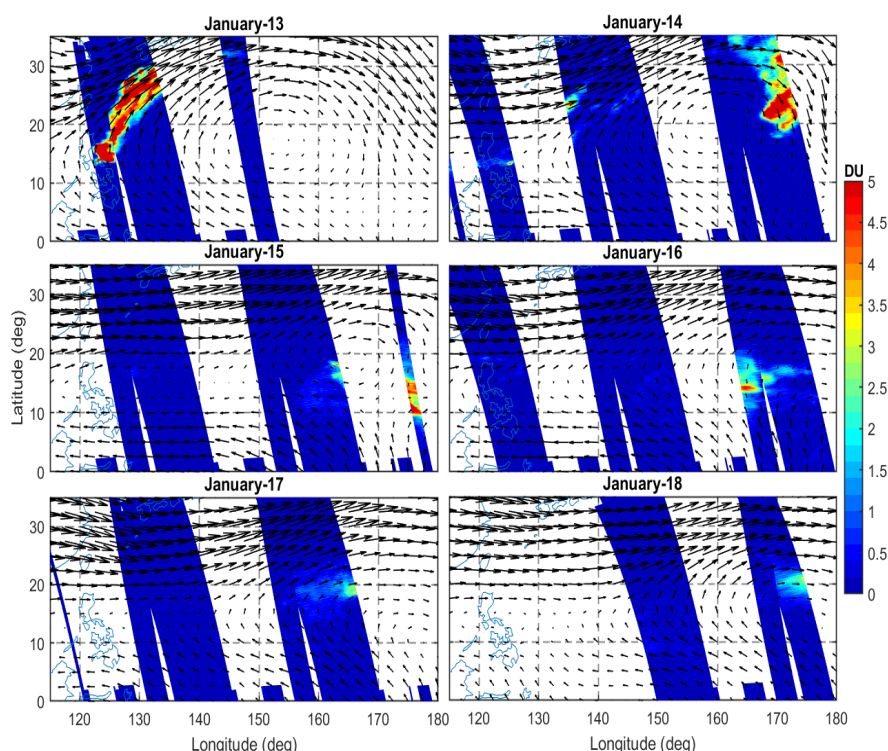
112 To geographically identify the area covered by volcanic plume, we used the
 113 operational product estimate of the column density of SO₂ for the middle tropospheric
 114 column (ColumnAmountSO₂_TRM) data from the Aura Ozone Monitoring Instrument
 115 (OMI). The Aura OMI retrieves the SO₂ data from Earthshine radiance in the
 116 wavelength range of 310.5–340 nm (Levelt et al., 2006). It gives the total number of
 117 SO₂ molecules in the entire atmospheric column above a unit area
 118 (https://disc.gsfc.nasa.gov/datasets/OMSO2e_V003/). Details of the retrieval technique
 119 are documented by Li et al. (2017). The standard deviation of TRM retrievals in
 120 background areas is about 0.3 DU at low and mid-latitudes. The middle tropospheric
 121 SO₂ column is corresponding to the center of mass altitude (CMA) of 8 km, generally
 122 recommended for use in studies on moderate eruptions and long-range transport of



Apart from above mentioned data, we also used daily mean NCEP reanalysis wind data during the Taal volcanic eruption. The NCEP wind data were downloaded from the following website <https://psl.noaa.gov/data/gridded/data.ncep.reanalysis.pressure.html>.

130 **3.1 SO2 observations**

6



148

149 **Figure 2.** Spatial distribution of middle tropospheric column (TRM) sulfur dioxide
 150 (SO_2) from Aura ozone monitoring instrument (OMI) for each day, 13-18 January 2020.
 151 (Unit: Dobson units; $1\text{DU} = 2.69 \times 10^{16} \text{ molecules cm}^{-2}$).

152 However, during the time period of 15 -18 January, the center of the anticyclone
 153 was strongly located over the region of 10-20N, 160-180E. The SO_2 observations from
 154 the OMI clearly exhibited a significant signal of the SO_2 within the anticyclone during
 155 15-18 January (**Figure 2**). We also observed significant SO_2 signal during 19 and 20
 156 January over this region with less magnitude (Figure not shown). Overall, the SO_2
 157 released from the Taal volcanic eruption in the afternoon on 12-13 January, transported
 158 through the upper level strong winds and into a strong anticyclone over the Pacific
 159 Ocean in northern hemisphere. This is quite interesting that the strong anticyclonic
 160 circulation at upper level plays a crucial role in transporting the SO_2 from the Taal
 161 volcanic eruption. In the following sections, the impact of this Taal injected SO_2 on the



temperature structure is discussed in detail.

3.3 Temperature structure during Taal volcanic eruption

It is clear that the Taal volcanic eruption started in the afternoon of 12 January and active throughout 13 January. The intensity of the eruption gradually decreased from 14 January and the eruption had dried up by the end of 15 January. Even significant eruption signals with less magnitude are detected over the Taal volcano after 15 January, the maximum SO_2 emission was recorded high on 13 January with measured value of ~5299 tones/day based on Philippine Institute of Volcanology and Seismology. It is expected that the atmospheric situations around the volcano varied due to the volcanic eruption. To see the temperature structure from the COSMIC-2 RO data, we selected 13 January as an intense volcanic eruption day.

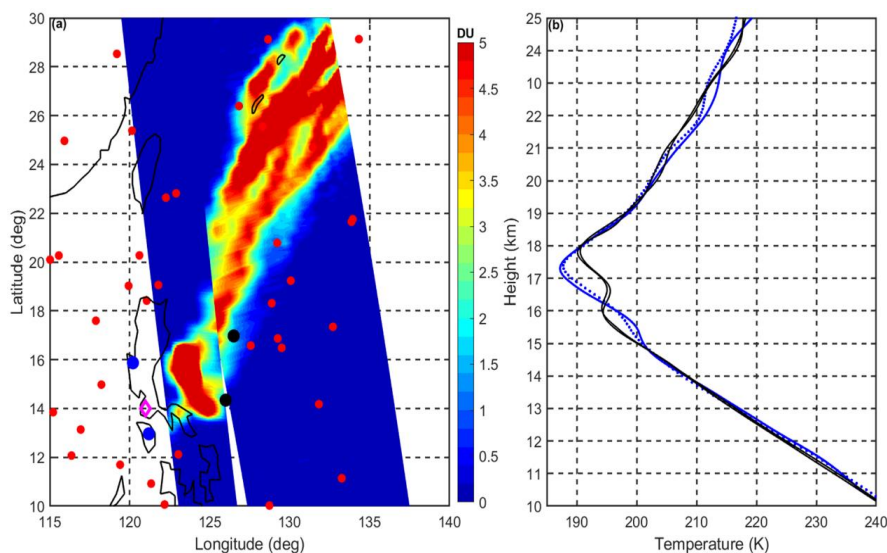


Figure 3. (a) Spatial distribution of COSMIC-2 RO profiles on 13 January around the area of Taal volcano. Magenta colored rectangle represents the location of the Taal volcano. Blue colored dots represent the nearest RO profiles to the volcano, and black dots represent the profiles away from the volcano; and (b) the corresponding temperature profiles for nearest and away regions from the volcano.



180 **Figure 3** shows the available RO data around the Taal volcano on 13 January along
181 with the OMI observed SO₂ data on the same day. The area of the Taal volcano is shown
182 by the magenta colored rectangle in the figure. On January 13, we found two
183 temperature profiles from COSMIC-2 RO data in the area of the eruption (within 200
184 km from the eruption center), highlighted in blue colored dots in the figure. Two more
185 temperature profiles are also detected away from the eruption center, significantly
186 affected by the volcanic plume (highlighted with black colored dots). The observed
187 vertical temperature profiles for near source region and away from the source region
188 are shown in **Figure 3b**.

189 It is very interesting that the vertical temperature structure is quite different from
190 around the center to away from the volcanic eruption. Between 10 and 15 km, the
191 temperature profiles exhibit similar structure, whereas above 15 km the temperature
192 profiles show different structure. Near the center of the eruption, the temperature
193 inversion was observed around 15 km and the cold point tropopause height is noticed
194 around 17 km altitude (blue colored profiles). However, away from the volcano, the
195 inversion started at 16 km altitude and the cold point tropopause height is detected
196 around 18 km. Also, ~5K difference is observed between the temperature profiles near
197 and away from the volcano at the tropopause during the active eruption period. This is
198 quite interesting and strongly evident that the multiple tropopauses are noticed in the
199 temperature profiles that are available away from the volcano center.

200 Similarly, we examined the vertical temperature structure within $\pm 5^\circ$ latitude and
201 longitude radius from the volcano center. In total, there are 14 temperature profiles
202 within the $\pm 5^\circ$ latitude and longitude around the volcano center on January 13 as shown
203 in **Figure 4a**. The corresponding observed vertical temperatures are shown in **Figure**
204 **4a**. From the **Figure 4a**, it is again evident that the temperature structure is quite
205 different from one to the others, particularly between 15 to 20 km altitude ranges. We



also detected the multiple tropopauses in most of the temperature profiles. To quantify the temperature changes in the active volcanic eruption day, we compared the temperature profiles available on 13 January with the mean temperature of a week before the eruption (here after background mean temperature). The background mean temperature is computed using all the temperature profiles during 5-11 January that are available within $\pm 5^\circ$ latitude and longitude radius from the volcano center. Finally, we subtracted all individual temperature profiles available on 13 January with the background mean temperature. The difference in the temperature profiles is shown in **Figure 4b**. The solid black colored line represents the mean of all the temperature difference profiles estimated by using the 14 profiles.

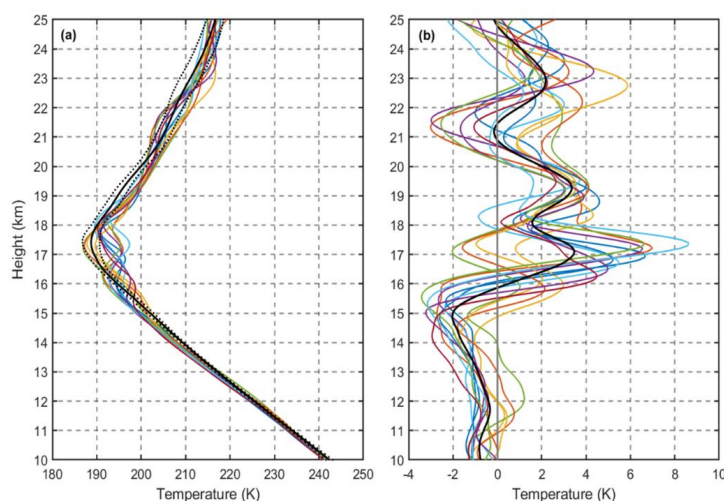


Figure 4. (a) Observed vertical temperature profiles on 13 January along with mean temperature (black) of one week before the eruption within the 5 degree radius from the Taal volcano, and (b) temperature difference of the available temperature profiles within the 5 degree radius for one week before the eruption. Black dotted lines showed in (a) are the standard deviation for the mean temperature of one week before the eruption.

From **Figure 4b**, it is clear that all the profiles exhibit significant negative temperature anomalies in the 10-15 km region. The mean of maximum negative temperature anomaly is noticed around 15 km altitude. The negative to positive changes



happened at around 16 km altitude. Further, most of the profiles exhibits positive temperature anomalies from 16 km altitude onwards. The maximum positive temperature anomaly is of about 3.5 K in the mean profile, and of up to ~8 K for individual profiles. It is also evident that there are two maxima positive anomaly locations around 17 km and 19 km. The observed positive temperature anomaly ~3.5 K in the upper atmosphere is well matched with previous studies (Wang et al., 2009; Biondi et al., 2017). Overall, from **Figure 4** we find clear evidence that the temperature structure after the volcanic eruption shows significantly different from those under normal conditions.

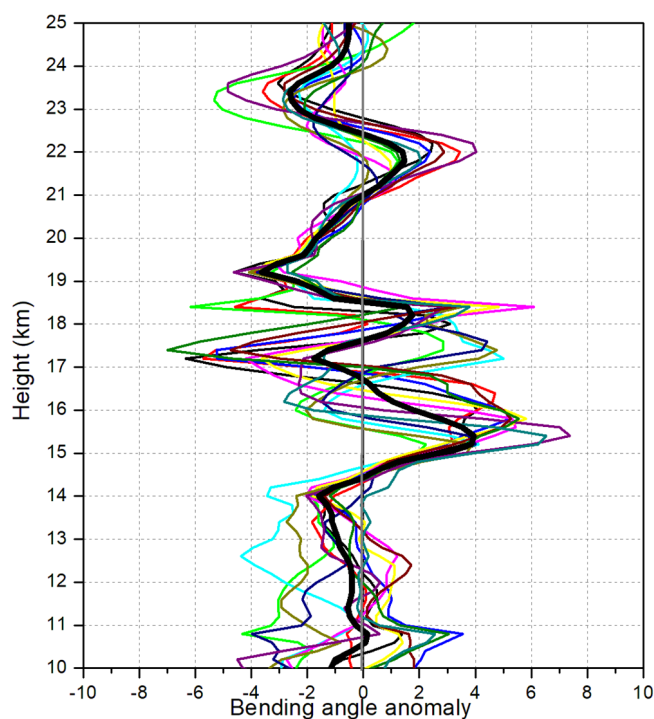


Figure 5. Standardized bending angle anomaly observed for the RO profiles available within 5 degree radius from the Taal volcano on 13 January. The anomaly is estimated with reference to the RO profiles available during one week before the eruption over the same region.



240 A few earlier studies clearly demonstrated the usefulness of RO technique for the
 241 detection of volcanic cloud top altitude by using bending angle anomaly method
 242 (Biondi et al., 2017; Cigala et al., 2019). In this study, the bending angle anomaly
 243 method was used to detect the cloud top altitude during the Taal volcanic eruption. The
 244 atmprf data from the COSMIC-2 was utilized. Its vertical resolution is 200 m. **Figure**
 245 **5** shows the standardized bending angle anomaly observed on 13 January 2020 within
 246 the degree radius from the volcano. The black colored solid line represents the mean of
 247 all 14 profiles. We estimated the bending angle anomaly with reference to the one week
 248 before the eruption over the same region. First, we subtracted the reference mean
 249 bending angle profile from the individual bending angle profiles around the volcano.
 250 The anomalies are further standardized with the reference data. A prominent peak in
 251 the bending angle anomaly defines the volcanic cloud top altitude. From the mean
 252 profile of bending angle anomaly (black colored solid line), the maximum peak is
 253 detected at 15.2 km. It is suggesting that the clouds reached the altitude of 15.2 km
 254 during the Taal volcanic eruption. This is quite different from the temperature
 255 anomalies shown in **Figure 4b**. The maximum positive temperature anomaly is noticed
 256 at ~17 km which is quite higher than the bending angle. Our study also further supports
 257 the detection of the cloud top altitude during the volcanic eruption.

258 We also investigated the tropopause changes due to this eruption. Changes in the
 259 different tropopause parameters over $\pm 5^\circ$ latitude and longitude around the area of the
 260 Taal volcano about 7 days before volcano eruption (5-11 January 2020) and just after
 261 the volcano eruption (12-15 January 2020) are investigated. **Table 1** shows the different
 262 tropopause parameters such as cold point tropopause height (CPT-H) and
 263 corresponding temperature (CPT-T), lapse rate tropopause height (LRT-H) and
 264 corresponding temperature (LRT-T), and convective tropopause height (COT-H) and
 265 the thickness of the tropical tropopause layer (TTL thickness), defined as the layer



266 between COT-H and CPT-H, for the Taal volcanic eruption that is observed before and
 267 just after the eruption. The COT-H is estimated by using the gradient in the potential
 268 temperature profile and the maximum gradient in the profile is identified as the COT-
 269 H (Ravindra Babu et al., 2015).

Tropopause Parameter	Before	After
CPT-H	17.6±0.5	17.2±0.4
CPT-T	188±2.1	189±1.7
LRT-H	17.1±0.4	16.9±0.5
LRT-T	188.4±2.4	189.3±2
COT-H	12.1±1.5	13.1±1.3
TTL thickness	5.5±1.7	4.1±1.4

270
 271 **Table 1.** Mean tropopause parameters observed for one week before the eruption and
 272 after the eruption. We considered 05-11 January period as one week before and 12-15
 273 January as an after the eruption period.

274 The CPT-H before the eruption around the Taal region is 17.6 km, whereas the
 275 LRT-H is 17.1 km with a standard deviation of 0.5 and 0.4 km, respectively. Just after
 276 the eruption, the CPT-H and LRT-H is slightly changed and the values are recorded as
 277 17.2±0.4 km and 16.9±0.5 km. There is a slightly decrease in the tropopause height just
 278 after the eruption. Similarly, the temperatures of tropopause (CPT-T and LRT-T) exhibit
 279 a significant increase in value by ~ 1K. The observed warmer tropopause temperatures
 280 are clear evidence for the presence of SO₂ around the tropopause region during the
 281 eruption period. Very interestingly the COT-H is increased by 1 km just after the
 282 eruption as compared with that before the eruption period, and this has led to the
 283 increase in the TTL thickness by 1.4 km after the eruption period. The observed strong
 284 increase in the COT-H is strongly due to the volcanic plume during the Taal eruption.



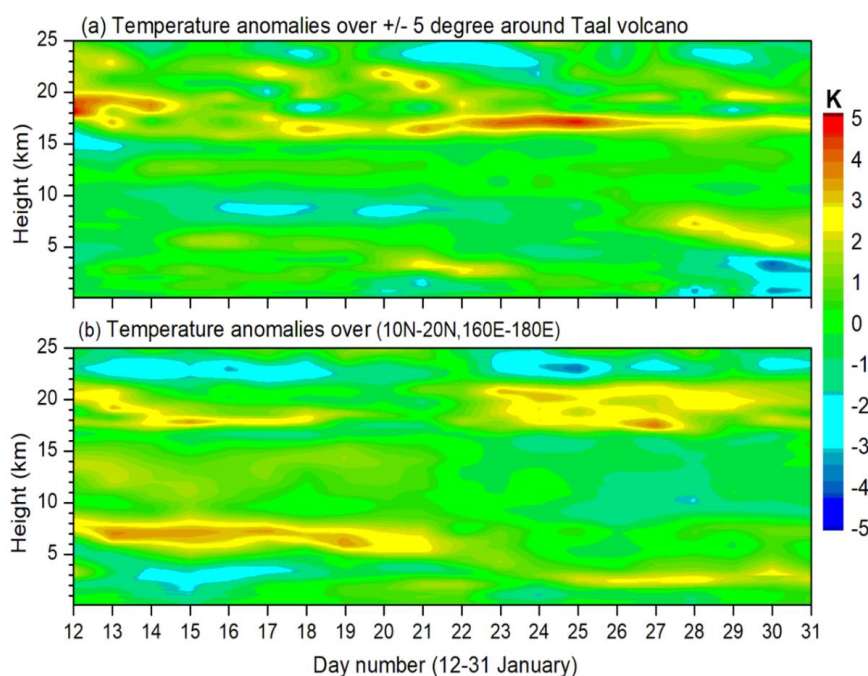
285 It is reported earlier that the plume of volcanic ash reached up to ~15 km over the Taal
286 volcano region during the eruption (Mallapaty et al., 2020).

287 **3.4 Diurnal variability in temperature and relative humidity**

288 The COSMIC-2 provides more than 5000 high vertical resolution temperature
289 profiles within a day over the tropics (Hu et al., 2020). This allows us to see the
290 significant diurnal changes in the basic atmospheric parameters, such as temperature
291 and relative humidity (RH). By utilizing this advantage, we investigated diurnal
292 variability in the atmospheric temperature and relative humidity after the eruption in
293 the study. Two regions were selected, within $\pm 5^\circ$ latitude and longitude radius from
294 the Taal volcano as one study region and the area between 10-20N, 160-180E as a
295 second study region. One can notice that first region has been the source region of SO₂
296 just around the volcanic eruption and another one is the away from the source region,
297 but the injected SO₂ from the eruption reached and accumulated over the second region
298 during the Taal eruption. In this way it is important to see how the atmosphere is
299 responded after the eruption over the two different regions. We carried out similar
300 analysis, which is mentioned in the previous sections. We subtracted the daily mean
301 temperatures during 12-31 January from the background temperature over the
302 respective regions. The observed temperature difference between the daily mean
303 temperature and background mean temperature over two regions are shown in **Figure**
304 **6**. The temperature anomaly shown in **Figures 6a and 6b** shows quite different
305 behavior over the two regions. The anomaly shown in **Figure 6a** indicates that a
306 persistent positive temperature anomaly is observed at 16-19 km altitude region in the
307 area around the Taal volcano and it is remained for several days after the eruption.
308 Whereas, over the Pacific region, the positive temperature anomaly is persisting up to
309 19 January, after that there was a noticeable drop in the positive temperature anomaly
310 for two to three days. Then again the positive temperature anomaly is persistent for the



311 next few days.



312
 313 **Figure 6.** Observed daily mean temperature anomalies over (a) ± 5 degree around the
 314 Taal volcano, and (b) region around 10-20N, 160-180E.
 315 The maximum warming over the Taal volcano region is observed at 18 km altitude
 316 on 13 January with the magnitude of ~ 4 K (**Figure 6a**). The temperature anomalies at
 317 17-19 km altitude range during 12-15 January significantly exhibit warmer compared
 318 to the remaining days (**Figure 6a**). We also noticed a significant negative temperature
 319 anomaly by about 2-3 K at 15 km altitude just after the eruption over the Taal volcano
 320 (**Figure 6a**). However, this feature does not appear over the Pacific region at the same
 321 altitude. This may be due to the sudden increase in the atmospheric water vapor at that
 322 altitude region. It is expected that large amount of water vapor is transported during the
 323 eruption period along with SO_2 . Over the Pacific region, a significant cooling of the
 324 lower stratosphere (22-25 km) is evident after the eruption. One interesting finding from
 325 the **Figure 6b** is that there is a layer of warming in the atmosphere around 5-20 km



altitude region. The significant warming in the troposphere might be due to the strong anticyclonic circulation associated with SO_2 from the eruption over the region during the eruption period. We also observed significant cooling of the mid troposphere over the Taal volcano region after the eruption (**Figure 6a**). Overall a warm anomaly of nearly 5 K at ~ 18 km just above the tropopause appears as the eruption signature over the Taal volcano. The persistent warming around the tropopause region appears after the eruption indicating the effect of SO_2 plume and its direct radiative effect induces a heating of the atmosphere around the tropopause. Overall, both locations show significant warming of the tropopause region, suggesting that both locations are influenced by the volcanic plume.

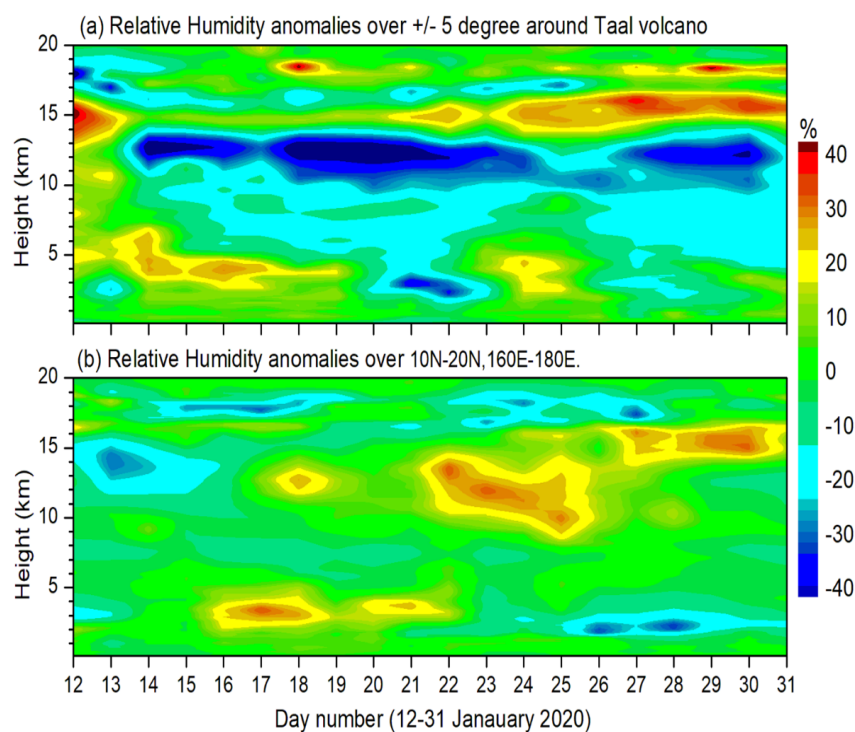


Figure 7. Observed daily mean relative humidity anomalies over (a) ± 5 degrees around the Taal volcano and (b) region around 10-20 N, 160-180 E.



339 Similarly, the diurnal variability in the RH is also investigated by using the
340 COMSIC-2 RO data and the observed anomalies are shown in **Figure 7**. Interestingly,
341 the anomalies observed in the RH over two regions exhibit quite different from one to
342 another. A significant increase in the RH is evident in the mid and upper troposphere
343 with the maximum increase noticed at ~15 km altitude on just after the eruption over
344 the Taal volcano region. While, in Pacific region, the RH shows a significant decrease
345 after the eruption at ~15 km altitude range (**Figure 7b**), we also observed a noticeable
346 decrease in the RH at ~17-19 km altitude over the Taal volcano region just after the
347 eruption (**Figure 7a**). Drying of the lower stratosphere due to the presence of SO₂ is
348 one of the prominent signatures of the volcanic eruption (Glaze et al., 1997). The
349 observed negative RH anomalies at ~17-19 km altitude over the Taal volcano region
350 and at ~15 km altitude over the Pacific region from the present study strongly support
351 the evidence of the eruption signatures. Both locations show significant negative RH
352 anomalies in the lower stratosphere after the eruption, suggesting that both locations
353 are influenced by the volcanic plume. After the eruption, the RH anomalies show
354 persistent decrease in the RH around the upper troposphere over the Taal volcano region.
355 This is expected that the SO₂ emitted from the volcano reacts with water vapor to
356 produce sulphate aerosols over a period of some weeks (Pinto et al., 1989). The
357 observed mid tropospheric negative temperature anomalies from **Figure 6a** after the
358 eruption over the Taal volcano region are mirrored in the troposphere drying, which is
359 noticed by the large lowering of the RH (**Figure 7a**). The RH is lowered by 50% after
360 the eruption from 14 January onwards over the Taal volcano region. Our results from
361 the RH observations from COSMIC-2 clearly show the volcano eruption signatures at
362 day-to-day time scales. It is reported that the impact of small volcanic eruptions on the
363 temperature changes is varied with respect to altitude and latitude (Stocker et al., 2019).
364 The present results are also in agreement with the previous reports. The temperature



365 and RH clearly exhibit different variability with respect to altitude (surface to 20 km)
366 and also quite different variability was noticed over source region and the receptor
367 region.

368 4. Conclusion

369 Very recently, on the afternoon of 12 January 2020, a large eruption occurred at
370 the Taal volcano located in the Philippines (14°N 120.59°E). This was the first time
371 since its previous eruption in 1977. However, this eruption during January 2020 was
372 active for a few days and it was weakened just after a few days. Though it injected a
373 significant amount of SO₂ into the atmosphere and within a few days the injected SO₂
374 transported towards the central Pacific Ocean in the northern hemisphere due to the
375 strong upper level winds. The injected SO₂ reached at about ~15 km during its active
376 eruption period. In the present study, we have analyzed the temperature structure and
377 its variability during and after the eruption. We used high resolution temperature
378 measurements from recently launched COSMIC-2 mission for the first time. As
379 COSMIC-2 provides a much higher number of temperature profiles compared to the
380 previous RO missions over the tropics in a single day, we examined the temperature
381 and also relative humidity changes due to the eruption at day-to-day scales. Previously,
382 few studies reported the temperature changes after the volcanic eruption by using a
383 small number of RO data (Wang et al., 2009; Okazaki and Heki, 2012). Wang et al.
384 (2009) and Okazaki and Heki, (2012) studied the eruptions occurred over the mid
385 latitude regions. However, they reported the instantaneous and localized temperature
386 changes associated with the eruptions. Biondi et al. (2017) firstly studied the volcanic
387 eruption over the tropics by using COSMIC RO data. They studied the Nabro eruption,
388 which occurred in June 2011 over the tropics. They reported the positive temperature
389 anomaly by about 4K in the mean, and up to 10 K for the individual profile in the UTLS



390 region. They considered $10^{\circ} \times 10^{\circ}$ latitude and longitude area around the Nabro volcano.
 391 In the present study, we considered the $5^{\circ} \times 5^{\circ}$ latitude and longitude area around the Tall
 392 volcano. Our findings of temperature anomaly by about 3.5 K in the mean profile, and
 393 up to ~ 8 K for the individual profile are in good agreement with the results of Biondi
 394 et al. (2017).

395 In the present study, we also describe the detailed temperature structure with
 396 respect to the distance from the volcano center during its active eruption day. Further,
 397 the day-to-day temperature and relative humidity changes over $\pm 5^{\circ}$ latitude and
 398 longitude radius from the volcanic center and over the affected region away from the
 399 volcano ($10\text{--}20^{\circ}$ N, $160\text{--}180^{\circ}$ E). We compared the temperature and RH with respect to
 400 the mean data of one week before the eruption when there was no volcanic eruption.
 401 The present results in day-to-day temperature and RH changes immediately after the
 402 eruption are the first of its kind of very shorter scales, which are not presented earlier.
 403 We found a clear warming signature in the lower stratosphere region due to the SO_2
 404 after the eruption of Taal with mean amplitudes about 5 K just after the eruption and
 405 persisting for the next two weeks. Overall, significant increased RH in the troposphere
 406 and lowering of the RH in the lower stratosphere along with the warming of the
 407 tropopause region due to the presence of SO_2 are the strong signatures of the Taal
 408 volcanic eruption. The major findings from the present study are summarized as follows

- 409 ● A significant temperature inversion at ~ 15 km altitude is observed in the nearest
 410 temperature profiles (within 2-degree radius). Multiple tropopauses are evident in
 411 the temperature profiles that are available away from the volcano (~ 5 -degree
 412 radius).
- 413 ● A ~ 3.5 K in the mean profile and up to ~ 8 K warming for individual profile was
 414 observed within $\pm 5^{\circ}$ latitude and longitude from the volcano center compared to
 415 one week before the eruption when there was no volcanic eruption on 13 January.



416 ● A persistent warming layer at 16-19 km altitude region is evident over the Taal
417 volcano region (Pacific region) and it is further remained for several days after the
418 eruption.

419 ● A significant increase (decrease) in the RH is evident in the mid and upper
420 troposphere with the maximum increase is noticed at ~15 km altitude on just after
421 the eruption over the Taal volcano region (Pacific region).

422 ● The present work shows the advantages and the usefulness of the COSMIC-2 data
423 for near real-time temperature monitoring at shorter time scales with higher
424 density of the data.

425 In recent period, the small volcanic eruption research has got immense interest in the
426 scientific community. Hence, several studies were reported on the impact of the small
427 volcanic eruptions on the atmospheric temperature (Wang et al., 2009; Okazaki and
428 Heki, 2012; Mehta et al., 2015; Stocker et al., 2019). Also, a contribution of those
429 eruptions to the 21st century warming hiatus has been discussed earlier (Santer et al.,
430 2015). To represent the comprehensive trends in the atmospheric temperatures, the
431 detailed knowledge and understanding of the vertical temperature structure is crucial
432 particularly during volcanic eruptions. The recently launched COSMIC-2 RO data
433 provide higher density of the finer temperature profiles over the tropics in a single day.
434 From the present study, it is concluded that the COMSIC-2 data is also suitable for
435 study the small scale variability in the atmospheric temperature and relative humidity
436 during different extreme events (volcanic eruptions, tropical cyclones etc.) particularly
437 over the tropics.

438 **Author contributions:** S. Ravindra Babu designed the study, conducted research,
439 performed complete data analysis and drafted the first manuscript. Y.-A. Liou edited
440 the first manuscript. S. Ravindra Babu and Y.-A. Liou finalized the manuscript for
441 communication with the journal.



442 **Competing interests:** The authors declare that they have no conflict of interest.

443

444 **Acknowledgments:** We thank the COSMIC Data Analysis and Archive Centre
445 (CDAAC) for providing COSMIC-2 provisional data used in the present study through
446 its FTP site (<http://cdaac-www.cosmic.ucar.edu/cdaac/products.html>). We also thank
447 NASA for providing the Aura Ozone Monitoring Instrument (OMI) data
448 (https://disc.gsfc.nasa.gov/datasets/OMSO2e_V003/). Thanks to NCEP for providing
449 the wind data. Appreciations are also due to the Ministry of Science and Technology
450 (MOST) of Taiwan for financial support through grants MOST 108-2111-M-008-036-
451 MY2 and 108-2923-M-008-002-MY3.

452 **Data Availability**

453 All the data used in the present study is available freely from the respective websites.
454 The COSMIC RO data is available from COSMIC CDAAC website ([http://cdaac-](http://cdaac-www.cosmic.ucar.edu/cdaac/products.html)
455 [www.cosmic.ucar.edu/cdaac/products.html](http://cdaac-www.cosmic.ucar.edu/cdaac/products.html)). The NCEP wind data available from
456 <https://psl.noaa.gov/data/gridded/data.ncep.reanalysis.pressure.html>. The Aura OMI
457 SO₂ data is freely available through
458 https://disc.gsfc.nasa.gov/datasets/OMSO2e_V003/.

459 **References**

460 Aquila, V., Oman, L. D., Stolarski, R., Douglass, A. R., and Newman, P. A.: The
461 Response of Ozone and Nitrogen Dioxide to the Eruption of Mt. Pinatubo at
462 Southern and Northern Midlatitudes, J. Atmos. Sci., 70, 894–900,
463 <https://doi.org/10.1175/JAS-D-12-0143.1>, 2013.

464 Biondi, R., Steiner, A. K., Kirchengast, G., Brenot, H., and Rieckh, T.: Supporting the
465 detection and monitoring of volcanic clouds: A promising new application of
466 Global Navigation Satellite System radio occultation, Adv. Sp. Res., 60, 2707–



- 2722, <https://doi.org/10.1016/j.asr.2017.06.039>, 2017.
- Cigala, V., Biondi, R., Prata, A.J., Steiner, A.K., Kirchengast, G., Brenot, H.: GNSS
 Radio Occultation Advances the Monitoring of Volcanic Clouds: The Case of the
 2008 Kasatochi Eruption, Remote Sens. 2019, 11, 2199,
<https://doi.org/10.3390/rs11192199>
- Free, M. and Lanzante, J.: Effect of volcanic eruptions on the vertical temperature
 profile in radiosonde data and climate models, J. Clim., 22, 2925–2939,
<https://doi.org/10.1175/2008JCLI2562.1>, 2009.
- Glaze, L. S., Baloga, S. M., and Wilson, L.: Transport of atmo-spheric water vapor by
 volcanic eruption columns, J. Geophys.Res., 102, 6099–6108, 1997.
- Ho et al. (2019) The COSMIC/FORMOSAT-3 radio occultation mission after 12 years:
 Accomplishments, remaining challenges, and potential impacts of COSMIC-2.
 Bull Amer Met Soc 100 online version:
<https://journals.ametsoc.org/doi/pdf/10.1175/BAMS-D-18-0290.1>
- Levelt, P. F., Oord, G. H. J. v. d., Dobber, M. R., Malkki, A., Huib, V., Johan de, V.,
 Stammes, P., Lundell, J. O. V., and Saari, H.: The ozone monitoring instrument,
 IEEE T. Geosci. Remote Sens., 44, 1093–1101,
<https://doi.org/10.1109/TGRS.2006.872333>, 2006.
- Li, C., Krotkov, N. A., Carn, S., Zhang, Y., Spurr, R. J. D., and Joiner, J.: New-
 generation NASA Aura Ozone Monitoring In-strument (OMI) volcanic
 SO₂ dataset: algorithm description, ini-tial results, and continuation with the
 Suomi-NPP Ozone Map-ping and Profiler Suite (OMPS), Atmos. Meas. Tech., 10,
 445–458, doi:10.5194/amt-10-445-2017, 2017.
- Mallapaty, S.: Scientists fear major volcanic eruption in the Philippines, Nature, 2020.



- 491 Mehta, S. K., Fujiwara, M., Tsuda, T., & Vernier, J. P. (2015). Effect of recent minor
 492 volcanic eruptions on temperatures in the upper troposphere and lower
 493 stratosphere. *Journal of Atmospheric and Solar-Terrestrial Physics*, 129, 99–110.
 494 <https://doi.org/10.1016/j.jastp.2015.04.009>
- 495 Okazaki, I. and Heki, K.: Atmospheric temperature changes by volcanic eruptions:
 496 GPS radio occultation observations in the 2010 Icelandic and 2011 Chilean cases,
 497 *J. Volcanol. Geoth. Res.*, 245–246, 123–127, 2012.
- 498 Parker, D. E., Wilson, H., Jones, P. D., Christy, J., and Folland, C.K.: The impact of
 499 Mount Pinatubo on climate, *Int. J. Climatol.*, 16, 487–497, .
 500 [https://doi.org/10.1002/\(SICI\)1097-0088](https://doi.org/10.1002/(SICI)1097-0088), 1996.
- 501 Pinto, J. P., Turco, R. P., and Toon, O. B.: Self-limiting physical and chemical effects in
 502 volcanic eruption clouds, *J. Geophys. Res.*, 94, 11165–
 503 11174, doi:10.1029/JD094iD08p11165, 1989.
- 504 Ramaswamy, V., Chanin, M. L., Angell, J., Barnett, J., Gaffen, D., Gelman, M.,
 505 Keckhut, P., Koshelkov, Y., Labitzke, K., Lin, J. J. R., O'Neill, A., Nash, J., Randel,
 506 W., Rood, R., Shine, K., Shiotani, M., and Swinbank, R.: Stratospheric
 507 temperature trends: Observations and model simulations, *Rev. Geophys.*, 39, 71–
 508 122, <https://doi.org/10.1029/1999rg000065>, 2001.
- 509 Randel, W. J., Garcia, R. R., Calvo, N., and Marsh, D.: ENSO influence on zonal mean
 510 temperature and ozone in the tropical lower stratosphere, *Geophys. Res. Lett.*, 36,
 511 1–5, <https://doi.org/10.1029/2009GL039343>, 2009.
- 512 RavindraBabu, S., VenkataRatnam, M., Basha, G., Krishnamurthy, B.V., and
 513 Venkateswararao, B.: Effect of tropical cyclones on tropical tropopause parameters
 514 observed using COSMIC GPS RO data. *Atmos. Chem. Phys.*, doi: 10.5194/acp-



- 515 15-1-2015, 2015.
- 516 Robock, A.: Volcanic eruptions and climate. *Reviews of Geophysics*, 38(2), 191–219.
- 517 <https://doi.org/10.1029/1998rg000054>, 2000.
- 518 Robock, A.: Climatic impacts of volcanic eruptions Edited by H. Sigurdsson (pp. 935–
- 519 942). <https://doi.org/10.1016/B978-0-12-385938-9.00053-5>, 2015.
- 520 Santer, B. D., Solomon, S., Bonfils, C., Zelinka, M. D., Painter, J. F., Beltran, F., et al.:
- 521 Observed multivariable signals of late 20th and early 21st century volcanic activity.
- 522 *Geophysical Research Letters*, 42, 500–509.
- 523 <https://doi.org/10.1002/2014GL062366>, 2015.
- 524 Stocker, M., Ladstädter, F., Wilhelmsen, H., and Steiner, A. K.: Quantifying
- 525 stratospheric temperature signals and climate imprints from post-2000 volcanic
- 526 eruptions. *Geophysical Research Letters*, 46, 12,486–12,494.
- 527 <https://doi.org/10.1029/2019GL084396>, 2019.
- 528 Vernier, J.-P., Thomason, L. W., Pommereau, J.-P., Bourassa, A. E., Pelon, J., Garnier,
- 529 A., Hauchecorne, A., Blanot, L., Trepte, C., Degenstein, D., and Vargas, F.: Major
- 530 influence of tropical volcanic eruptions on the stratospheric aerosol layer during the
- 531 last decade, *Geophys. Res. Lett.*, 38,
- 532 L12807, <https://doi.org/10.1029/2011GL047563>, 2011.
- 533 Wang, K.Y., Lin, S.C., Lee, L.C.: Immediate impact of the Mt Chaiten eruption on
- 534 atmosphere from FORMOSAT-3/COSMIC constellation. *Geophys. Res. Lett.* 36,
- 535 L03808, 2009.
- 536